

# Design and Analysis of Channel-Phase-Precoded Ultra Wideband (CPPUWB) Systems

Yu-Hao Chang, Shang-Ho Tsai, Xiaoli Yu and C.-C. Jay Kuo  
Department of Electrical Engineering  
University of Southern California, Los Angeles, CA 90089-2564, USA  
E-mails: {yuhaocha,shanghot,xiaoliyu}@usc.edu and cckuo@sipi.usc.edu

**Abstract**—A new indoor data communication scheme called the channel phase precoded ultra wideband (CPPUWB) system is proposed in this work. The proposed CPPUWB system is efficient in computational power saving by encoding the transmit symbol with a channelized codeword. The channelized codeword is determined by the channel phase information that is estimated at the receiver and then fed back to the transmitter. A method to estimate the channel phase information using training symbols is presented. For a given number of training symbols, we derive a lower bound for the average output SNR, which can be used to evaluate the system performance. Finally, an MMSE receiver is proposed to suppress the residual intersymbol interference (ISI) for the high data rate scenario.

## I. INTRODUCTION

The ultra-wideband (UWB) communication system enjoys a large multipath diversity gain owing to its high time-domain resolution. On one hand, the large number of multiple paths can effectively combat channel fading since the probability of all paths suffering from deep fading simultaneously is low. On the other hand, the fine temporal resolution leads to serious inter-symbol-interference (ISI) that makes channel equalization challenging. It was shown in [1] that tens or even hundreds of correlation operations are demanded to yield a satisfactory multipath diversity gain. A receiver with a large number of correlation operations demands a high computational power, which imposes a severe constraint on the receiver design.

The time-reversal prefiltering (TRP) technique, originated from underwater acoustic signal processing, was adopted by Strohmer *et al.* [2] to reduce the number of correlation operations in the receiver of an UWB system. That is, if the channel impulse response (CIR) is available at the transmitter, the time-reversed version of CIR is chosen to be the impulse response of the prefilter. It was shown in [2] that the use of TRP leads to signal power concentration at the desired receiver, which not only reduces the number of correlation operators but also achieves a higher data rate and lower interference to other users.

However, there are several drawbacks of TRP. First, since an UWB channel may contain hundreds of taps, it is somewhat impractical for the receiver to pass the whole channel

information back to the transmitter. Second, the accuracy of channel estimation affects the system performance greatly. The complexity for UWB channel estimation is pretty high while the result is often not perfect [3]. Since a low cost device is not able to estimate the channel condition accurately, it degrades the TRP performance.

In this work, we propose a new transceiver architecture called the channel phase precoded UWB (CPPUWB) system to overcome the shortcomings of TRP. The channel phase information is chosen to be the sign of tap coefficients, which takes values of +1 or -1, in our system. If the binary phase information is available at the transmitter, the pre-coder uses the unit-power, time-reversed order of this binary phase sequence as the channelized codeword for data symbol coding. Then, we can observe a strong peak in the received signal since all multipath components are coherently summed. To decode the transmit data, we simply sample the received peak signal for decision making.

There are several features of the proposed CPPUWB system. Since the CPP system demands the receiver to estimate and feed back the signs of channel tap coefficients only (rather than the complete channel impulse response), its complexity is significantly lower than that of TRP. At the transmitter end, a more expensive linear amplifier is needed in TRP to provide a larger signal dynamic range as compared with CPP. At the receiver end, CPPUWB does not perform the despreading operation so that its hardware implementation is simpler and power consumption is lower. Furthermore, CPPUWB can be potentially used in high data rate transmission and secure data communication. These features will be detailed in Sec. IV.

A similar idea called delay tuning was proposed in [4], where the received signal power for the time-hopping UWB (THUWB) system is concentrated by properly adjusting the delay and phase of the transmitted signal. The proposed CPPUWB system is different from delay tuning in several aspects. First, the tap delay in the channel model used in [4] is random, which complicates the channel estimation and the received signal power focusing. Based on the equal-distance, tap-delay line UWB channel model in [5], we are able to develop an efficient channelized codeword. Second, our system allows a faster data rate transmission without much ISI penalty since the received power is more concentrated. In contrast, the fixed length time-hopping code in [4] does not exploit the received signal power concentration fully for higher data rate transmission.

<sup>1</sup>The research has been funded by the Integrated Media Systems Center, a National Science Foundation Engineering Research Center, Cooperative Agreement No. EEC-9529152. Any Opinions, findings and conclusions or recommendations expressed in this material are those of the authors and do not necessarily reflect those of the National Science Foundation.

The rest of the paper is organized as follows. The model of the CPPUWB system is presented in Sec. II. Then, the performance of the proposed CPPUWB system is analyzed in Sec. III, where three different cases are considered. They are systems with perfect phase estimation, imperfect phase estimation, and high rate transmission. A lower bound on the output SNR are derived to evaluate the system performance for a fixed number of training symbols. Also, the minimum mean square error (MMSE) receiver is proposed to suppress the residual ISI at the cost of increased receiver complexity when the data rate is high. The advantages of the CPPUWB system are discussed in Sec. IV. Simulation results are given in Sec. V to corroborate the derived theoretical results. As demonstrated in the simulation, the proposed system renders a similar performance as a direct-sequence UWB (DSUWB) system with 15 RAKE fingers at a much lower computational complexity. Finally, concluding remarks are drawn in Sec. VI.

## II. SYSTEM MODEL

The proposed CPPUWB system targets on the single-user indoor data communication environment, where a short-range high-data-rate communication technique based on the UWB technology [6] is of great interest. The block diagram of the proposed system is shown in Fig. 1. They are detailed below.

The carrierless UWB channel model proposed by Chao and Scholtz [7] is considered in this work. It can be written as

$$h(t) = \sum_{i=0}^{L-1} h_i \delta(t - i\Delta) = \sum_{i=0}^{L-1} p_i \alpha_i \delta(t - i\Delta), \quad (1)$$

where  $h_i = p_i \alpha_i$ ,  $L$  is the total number of paths,  $\Delta$  is the multipath resolution that is assumed to be the same as the time domain pulse width,  $p_i \in \{+1, -1\}$  with an equal probability is the phase information of the  $i$ th path, and  $\alpha_i$  is the corresponding amplitude. Usually,  $\alpha_i$  is modeled as an independent Rayleigh random variable with the following probability density function (PDF)

$$f_{\alpha_i}(x) = \frac{x}{\sigma_i^2} e^{-x^2/2\sigma_i^2}.$$

The average power of  $\alpha_i$ , which is equal to  $2\sigma_i^2$ , decays exponentially with index  $i$ , *i.e.*,

$$E\{\alpha_i^2\} = 2\sigma_i^2 = \Omega\gamma^i,$$

where  $E\{\cdot\}$  is the expectation operator,  $\Omega$  is the average power of  $\alpha_0$  and  $\gamma \equiv e^{-\Delta/\Gamma}$  where  $\Gamma$  is the decay time constant. Usually, we have  $\Gamma > \Delta$ .

At the first step, the receiver estimates the carrierless channel phase information, which is either  $+1$  or  $-1$  for each tap. Then, the estimated channel phase information  $\hat{\mathbf{p}}$  is fed back to the transmitter and used as a channelized codeword  $\mathbf{c}$ , which is normalized to be with an unit power. Specifically, we choose

$$\mathbf{c} = [c_0, \dots, c_{L-1}]^T = \frac{1}{\sqrt{L}}[\hat{p}_{L-1}, \dots, \hat{p}_0]^T,$$

where  $L$  is the number of chips in  $\mathbf{c}$  and the superscript  $T$  denotes the matrix transpose. At the second step, the transmitter encodes each of the bipolar data symbol,  $b(i)$ , by

the channelized codeword. A pulse generator modulates the UWB pulse waveform  $w_s(t)$  onto each chip. Mathematically, the transmit signal can be expressed as

$$x_s(t) = \sum_{i=-\infty}^{\infty} b(i) \sum_{j=0}^{L-1} c_j w_s(t - j\Delta - iT_s),$$

where  $b(i) \in \{+1, -1\}$  is the  $i$ th bipolar signal,  $w_s(t)$  is the transmit pulse waveform, and  $T_s$  is the symbol interval, which is properly chosen to reduce ISI.

Based on the channel model in (1), the discrete received signal for the  $i$ th data symbol  $b(i)$  after chip-matched filtering and sampling can be written as

$$\mathbf{r}(i) = [r_0(i), \dots, r_{2L-2}(i)]^T = \mathbf{H}\mathbf{c}b(i) + \mathbf{I}(i) + \mathbf{n}(i), \quad (2)$$

where  $\mathbf{H}$  is a  $(2L - 1) \times L$  Toeplitz matrix whose first column contains  $\mathbf{h} = [h_0, \dots, h_{L-1}]^T$  from the first to the  $L$ th elements and zeros elsewhere,  $\mathbf{I}(i) = [I_0(i), \dots, I_{2L-2}(i)]^T$  is the interference vector that contains ISI, and  $\mathbf{n}(i) = [n_0(i), \dots, n_{2L-2}(i)]^T$  is the additive white Gaussian noise (AWGN) vector with zero mean and covariance matrix  $\frac{N_0}{2}\mathbf{I}_{2L-1}$ , where  $\mathbf{I}_{2L-1}$  is the  $(2L - 1) \times (2L - 1)$  identity matrix.

Let  $\bar{\mathbf{h}} = [\bar{h}_0, \dots, \bar{h}_{2L-2}]^T = \mathbf{H}\mathbf{c}$ . When the phase estimation is perfect, *i.e.*,  $\mathbf{p} = \hat{\mathbf{p}}$ , we have

$$\max_j \bar{h}_j = \sum_{i=0}^{L-1} \frac{\alpha_i}{\sqrt{L}} \quad (3)$$

at  $j = L - 1$  since all channel taps are coherently combined. To detect transmit symbol  $b(i)$  at the receiver, we simply apply the decision rule to  $r_{L-1}(i)$  in (2), *i.e.*,

$$\hat{b}(i) = \text{sign}\{r_{L-1}(i)\}.$$

It is worthwhile to comment that the maximum ratio combining (MRC) scheme that combines the peak as well as off-peak received signals for the same transmit symbol can be used by the receiver to enhance the output SNR. However, since the amplitude information is needed in MRC, additional training symbols will be demanded for the amplitude estimation and the computational cost will increase accordingly. Thus, we do not pursue along this direction in this work.

## III. PERFORMANCE ANALYSIS OF CPPUWB SYSTEM

In this section, we analyze the performance of the proposed CPPUWB system in terms of the signal-to-interference-plus-noise-ratio (SINR). Three different cases are considered. In the first case, we assume that there is no phase mismatch and the received signal  $r_{L-1}(i)$  used to decode  $b(i)$  contains no interference, *i.e.*,  $T_s \geq L\Delta$ . The output SINR obtained in this case provides a performance benchmark for the other two cases. In the second case, we consider the situation where the phase estimation is not perfect. More training symbols will result in more accurate phase estimation at the cost of the training overhead. Thus, it is important to analyze the relationship between the number of training symbols and the achievable performance. For a fixed number of training symbols without interference, we derive a lower bound on

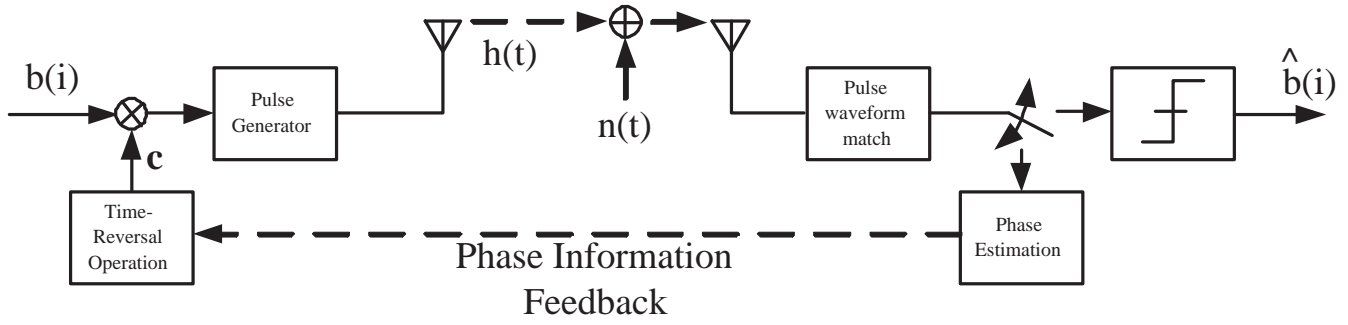


Fig. 1. The block diagram of the proposed CPPUWB system.

the average output SNR of the detected signal  $r_{L-1}(i)$  to evaluate the system performance. This lower bound specifies the maximum number of training symbols needed to achieve an output SNR for channel phase estimation. In the third case, we show how the system performance degrades as the data rate increases, *i.e.*, the channelized codewords of different symbols may overlap to result in ISI. Although CPPUWB can mitigate ISI to a certain degree, simulation results in Sec. V show that the ISI effect is large when the data rate is high. For this case, we suggest to use the MMSE receiver for ISI suppression. Note that there is no interference in the first and the second cases, and we also assume that the received signal is synchronized before phase estimation takes place.

#### A. Case I: Perfect Phase Information

Here, we consider the case where  $\hat{\mathbf{p}} = \mathbf{p}$  and  $r_{L-1}(i)$  is ISI-free, *i.e.*,  $T_s > L\Delta$ . The  $i$ th symbol of the received signal under detection can be written as

$$\begin{aligned} r_{L-1}(i) &= \frac{1}{\sqrt{L}} \sum_{l=0}^{L-1} \hat{p}_l p_l \alpha_l b(i) + n_{L-1}(i) \\ &= \frac{1}{\sqrt{L}} \sum_{l=0}^{L-1} \alpha_l b(i) + n_{L-1}(i). \end{aligned}$$

The average output SNR can be found as

$$\begin{aligned} \bar{\nu} &= \frac{E \left\{ \left( \frac{1}{\sqrt{L}} \sum_{l=0}^{L-1} \alpha_l b(i) \right)^2 \right\}}{E \{ n_{L-1}(i)^2 \}} \\ &= \frac{2}{LN_0} \left\{ \left( 1 - \frac{\pi}{4} \right) \Omega \frac{1 - \gamma^L}{1 - \gamma} + \frac{\pi\Omega}{4} \left( \frac{1 - \gamma^{L/2}}{1 - \gamma^{1/2}} \right)^2 \right\} \\ &\approx \frac{2}{LN_0} \left\{ \Omega \frac{1 - \pi/4}{1 - \gamma} + \frac{\pi\Omega}{4} \left( \frac{1}{1 - \gamma^{1/2}} \right)^2 \right\}, \end{aligned}$$

where the above approximation is obtained using  $\gamma^L \approx 0$  since  $\gamma < 1$  and  $L$  is large. The average output SNR derived above serves as an upper bound for the following two cases since it has perfect phase knowledge and there is no ISI.

#### B. Case II: Imperfect Phase Estimation

Phase estimation is usually not perfect in practice. A simple phase estimation scheme can be implemented as follows. During the channel initialization,  $N$  training symbols with a

low duty cycle,  $b_t(0), \dots, b_t(N-1)$ , are transmitted such that the received signal is free from ISI. The receiver matches the received pulse waveform and then takes samples at the chip rate to get the discrete data for phase estimation. All  $N$  discrete received signals are first demodulated and then averaged out to reduce the noise effect before phase estimation. The estimated phase  $\hat{\mathbf{p}}$  can be acquired by

$$\begin{aligned} \hat{\mathbf{p}} &= \text{sign} \left\{ \frac{1}{N} \sum_{l=0}^{N-1} b_t(l) \mathbf{r}_t(l) \right\} \\ &= \text{sign} \left\{ \frac{1}{N} \sum_{l=0}^{N-1} b_t(l) (\mathbf{h} b_t(l) + \mathbf{n}_t(l)) \right\} \\ &= \text{sign} \left\{ \mathbf{h} + \mathbf{n}_t^{(N)} \right\}, \end{aligned} \quad (4)$$

where  $\mathbf{h} = [p_0 \alpha_0, \dots, p_{L-1} \alpha_{L-1}]^T$ ,  $\mathbf{r}_t(l)$  and  $\mathbf{n}_t(l)$  are the corresponding  $l$ th discrete received signal and noise vectors, respectively. The noise vector is modelled as an AWGN vector whose elements are zero-mean independent random variables with variance  $\frac{N_0}{2}$ . Thus, we have

$$\mathbf{n}_t^{(N)} \equiv \frac{1}{N} \sum_{l=0}^{N-1} \mathbf{n}_t(l) b_t(l) = [n_{t,0}^{(N)}, \dots, n_{t,L-1}^{(N)}]^T,$$

which is a zero-mean Gaussian random vector with covariance matrix equal to  $\frac{N_0}{2N} \mathbf{I}_L$ . A feedback channel is used to send the estimated phase information back to the transmitter after the phase estimation task is done. To simplify our analysis, a perfect feedback channel is assumed so that the phase error is only due to the estimation error at the receiver.

To evaluate the system performance in terms of the number  $N$  of training symbols, we can derive a lower bound for the output SNR of the phase estimate as follows. Let us define a new variable  $\rho_i \equiv p_i \hat{p}_i$ . Since

$$\begin{cases} \hat{p}_i = p_i & \Leftrightarrow & \rho_i = 1 \\ \hat{p}_i \neq p_i & \Leftrightarrow & \rho_i = -1, \end{cases}$$

$\rho_i$  can be used as an indicator about whether the  $i$ th estimated phase is correct or wrong.

The average signal power concentrated at the peak can be

written as

$$\begin{aligned}
& E \left\{ \left( \frac{1}{\sqrt{L}} \sum_{i=0}^{L-1} \rho_i \alpha_i b(i) \right)^2 \right\} \\
&= \frac{1}{L} E \left\{ \sum_{i=0}^{L-1} \alpha_i^2 \right\} + \frac{1}{L} E \left\{ \sum_{i,j=0; i \neq j}^{L-1} \rho_i \alpha_i \rho_j \alpha_j \right\} \\
&= \frac{1}{L} \sum_{i=0}^{L-1} \Omega \gamma^i + \frac{1}{L} \sum_{i,j=0; i \neq j}^{L-1} E\{\rho_i \alpha_i\} E\{\rho_j \alpha_j\}. \quad (5)
\end{aligned}$$

If the phase is estimated by (4), we can get the conditional probability for  $\rho_i$  as

$$\begin{aligned}
Pr\{\rho_i = -1 | \alpha_i\} &= Pr\{\alpha_i + n_{t,i}^{(N)} < 0 | p_i = 1; \alpha_i\} \\
&= Q\left(\sqrt{2N\alpha_i^2/N_0}\right), \\
Pr\{\rho_i = 1 | \alpha_i\} &= 1 - Pr\{\rho_i = -1 | \alpha_i\} \\
&= 1 - Q\left(\sqrt{2N\alpha_i^2/N_0}\right),
\end{aligned}$$

where  $n_{t,i}^{(N)}$  is the  $i$ th element of  $\mathbf{n}_t^{(N)}$  and

$$Q(x) \equiv \int_x^\infty \frac{1}{\sqrt{2\pi}} e^{-t^2/2} dt.$$

Therefore, we can simplify  $E\{\rho_i \alpha_i | \alpha_i\}$  as

$$\begin{aligned}
E\{\rho_i \alpha_i | \alpha_i\} &= Pr\{\rho = 1 | \alpha_i\} \cdot \alpha_i - Pr\{\rho = -1 | \alpha_i\} \cdot \alpha_i \\
&= \alpha_i - 2Q\left(\sqrt{2N\alpha_i^2/N_0}\right) \alpha_i.
\end{aligned}$$

Then, we have

$$\begin{aligned}
E\{\rho_i \alpha_i\} &= E_{\alpha_i} \{E\{\rho_i \alpha_i | \alpha_i\}\} \\
&= E\{\alpha_i\} - 2 \int_0^\infty Q\left(\sqrt{2Nx^2/N_0}\right) x f_{\alpha_i}(x) dx \\
&\geq E\{\alpha_i\} - \int_0^\infty e^{-Nx^2/N_0} x f_{\alpha_i}(x) dx, \quad (6)
\end{aligned}$$

where the inequality is due to the fact that [8]

$$Q(x) \leq \frac{1}{2} e^{-x^2/2}.$$

After some manipulations, (6) can be written as

$$E\{\rho_i \alpha_i\} \geq \frac{\sqrt{\pi\Omega}}{2} \gamma^{i/2} - \frac{\sqrt{2\pi}}{\Omega \gamma^i} \left( \frac{\Omega N_0 \gamma^i}{2N_0 + 2N\Omega \gamma^i} \right)^{3/2}. \quad (7)$$

Therefore, by substituting (7) into (5), the average output SNR can be bounded as

$$\begin{aligned}
\bar{\nu} &= \frac{E\left\{\left(\frac{1}{\sqrt{L}} \sum_{i=0}^{L-1} \rho_i \alpha_i b(i)\right)^2\right\}}{E\{n_{L-1}(l)^2\}} \\
&\geq \frac{2}{LN_0} \left\{ \Omega \frac{1-\gamma^L}{1-\gamma} + \sum_{i \neq j} \left[ \frac{\sqrt{\pi\Omega}}{2} \gamma^{i/2} - \frac{\sqrt{2\pi}}{\Omega \gamma^i} \left( \frac{\Omega N_0 \gamma^i}{2N_0 + 2N\Omega \gamma^i} \right)^{3/2} \right] \right. \\
&\quad \left. \cdot \left[ \frac{\sqrt{\pi\Omega}}{2} \gamma^{j/2} - \frac{\sqrt{2\pi}}{\Omega \gamma^j} \left( \frac{\Omega N_0 \gamma^j}{2N_0 + 2N\Omega \gamma^j} \right)^{3/2} \right] \right\}.
\end{aligned}$$

### C. Case III: Imperfect Phase Estimation plus ISI

When symbol interval  $T_s$  is less than the length of the channel response, there is an ISI effect resulting from the contribution of the previous and the next symbols to the peak of the current received symbol. Thus, the system performance degrades. To simplify the following discussion, we consider the case where the symbol interval is an integer multiple of the chip interval, *i.e.*,  $T_s = M\Delta$ , where  $M$  is a positive integer less than  $L$ . The received signal  $r_{L-1}(i)$  contaminated by ISI can be represented as

$$\begin{aligned}
r_{L-1}(i) &= \bar{h}_{L-1} b(i) + n_{L-1}(i) \\
&\quad + \sum_{j=1}^{\lfloor L/M \rfloor} \{\bar{h}_{L-1-jM} b(i+j) + \bar{h}_{L-1+jM} b(i-j)\},
\end{aligned}$$

where  $\lfloor x \rfloor$  is the floor function of  $x$  and  $b(i+j)$  and  $b(i-j)$  are the post-cursor and pre-cursor ISI for  $b(i)$ , respectively. It can be shown that

$$\bar{h}_k = \sum_{i=L_1}^{L_2} p_i c_{k-i} \alpha_i = \sum_{i=L_1}^{L_2} p_i \hat{p}_{L-1-k+i} \alpha_i,$$

where  $L_1 = \max\{0, k-L+1\}$  and  $L_2 = \min\{L-1, k\}$ . Furthermore, the average power of  $\bar{h}_k$  for  $k \neq L-1$  is

$$\begin{aligned}
E\{\bar{h}_k^2\} &= E\left\{\left(\sum_{i=L_1}^{L_2} p_i \hat{p}_{L-1-k+i} \alpha_i\right)^2\right\} = \sum_{i=L_1}^{L_2} E\{\alpha_i^2\} \\
&= \sum_{i=L_1}^{L_2} \Omega \gamma^i = \Omega \gamma^{L_1} \frac{1-\gamma^{L_2-L_1+1}}{1-\gamma}.
\end{aligned}$$

The average output SINR is equal to

$$\bar{\nu} = \frac{E\{\bar{h}_{L-1}^2\}}{N_0/2 + \sum_{j=1}^{\lfloor L/M \rfloor} E\{\bar{h}_{L-1-jM}^2\} + E\{\bar{h}_{L-1+jM}^2\}}.$$

By applying a similar approach used in Sec. III-B, we can find the lower bound of  $\bar{\nu}$  when the estimated phase is utilized as

$$\begin{aligned}
\bar{\nu} &\geq \frac{1}{L} \left\{ \Omega \frac{1-\gamma^L}{1-\gamma} + \sum_{i \neq j} \left[ \frac{\sqrt{\pi\Omega}}{2} \gamma^{i/2} - \frac{\sqrt{2\pi}}{\Omega \gamma^i} \left( \frac{\Omega N_0 \gamma^i}{2N_0 + 2N\Omega \gamma^i} \right)^{3/2} \right] \right. \\
&\quad \left. \cdot \left[ \frac{\sqrt{\pi\Omega}}{2} \gamma^{j/2} - \frac{\sqrt{2\pi}}{\Omega \gamma^j} \left( \frac{\Omega N_0 \gamma^j}{2N_0 + 2N\Omega \gamma^j} \right)^{3/2} \right] \right\} \\
&\quad \cdot \left( N_0/2 + \sum_{j=1}^{\lfloor L/M \rfloor} E\{\bar{h}_{L-1-jM}^2\} + E\{\bar{h}_{L-1+jM}^2\} \right)^{-1}.
\end{aligned}$$

As the data rate increases, the system performance degrades since more neighboring symbols overlap with each other, which leads to more serious ISI. In this case, the receiver proposed in Sec. II may not suppress ISI efficiently. Then, we may resort to an MMSE receiver to suppress the residual ISI furthermore. If the symbol interval is fixed, a shorter channel model used to describe the input-output relationship between  $r_{L-1}(i)$  and  $b(i)$  for all  $i$  can be expressed as

$$\tilde{h}(t) = \sum_{i=-\lfloor L/M \rfloor}^{\lfloor L/M \rfloor} \tilde{h}_i \delta(t - (L-1)\Delta - iT_s),$$

where  $\tilde{h}_i = \bar{h}_{L-1+iM}$ . A matrix representation for the input-output relation is

$$\tilde{\mathbf{r}}(i) = \tilde{\mathbf{H}}\mathbf{b}(i) + \tilde{\mathbf{n}}(i),$$

where

$$\tilde{\mathbf{H}} = \begin{bmatrix} \tilde{h}_{\lfloor L/M \rfloor} & \cdots & \tilde{h}_{-\lfloor L/M \rfloor} & \mathbf{0} \\ & \ddots & \ddots & \\ \mathbf{0} & & \tilde{h}_{\lfloor L/M \rfloor} & \cdots & \tilde{h}_{-\lfloor L/M \rfloor} \end{bmatrix},$$

$\mathbf{b}(i) = [b(i - 2\lfloor L/M \rfloor), \dots, b(i), \dots, b(i + 2\lfloor L/M \rfloor)]^T$ , and  $\tilde{\mathbf{r}}(i)$  and  $\tilde{\mathbf{n}}(i)$  are the corresponding received signal and noise, respectively.

The MMSE estimator for symbol  $b(i)$  can be constructed as

$$\mathbf{w} = \mathbf{R}_{\tilde{\mathbf{r}}}^{-1} \tilde{\mathbf{h}},$$

where  $\tilde{\mathbf{h}} = E\{\tilde{\mathbf{r}}(i)b(i)\} = [\tilde{h}_{-\lfloor L/M \rfloor}, \dots, \tilde{h}_{\lfloor L/M \rfloor}]^T$  and  $\mathbf{R}_{\tilde{\mathbf{r}}} = E\{\tilde{\mathbf{r}}(i)\tilde{\mathbf{r}}(i)^T\} = \tilde{\mathbf{H}}\tilde{\mathbf{H}}^T + \frac{N_0}{2}\mathbf{I}_{2\lfloor L/M \rfloor+1}$ . Thus, the  $i$ th estimated symbol  $\hat{b}(i)$  is given by

$$\hat{b}(i) = \text{sign}\{\mathbf{w}^T \tilde{\mathbf{r}}(i)\}.$$

Note that estimate  $\tilde{\mathbf{h}}$  can be obtained using another set of training symbols. The construction of this MMSE receiver assumes that the transmit data experiences a slow fading channel such that the duration of the data block size is much smaller than the channel time constant.

#### IV. FEATURES OF PROPOSED CPPUWB SYSTEMS

There are several major features associated with the proposed CPPUWB system, which are detailed below.

- **Low phase estimation complexity and feedback bandwidth**

Due to the large number of multipath components in an UWB channel, the complexity in channel estimation is higher [3] and the bandwidth of the feedback channel is larger. For the proposed CPPUWB system, the receiver can simply estimate the channel phase information; namely, the sign of the tap coefficient. The complexity in estimation is greatly reduced. Furthermore, it takes only one bit to represent the phase information of each channel tap in the feedback channel.

- **Power-efficient transceiver design**

The transceiver design in CPPUWB is simpler and more power efficient as compared with TRP-UWB. At the transmitter end, a data symbol is spread and prefiltered before transmission in TRP-UWB, where the prefiltering operation convolves the time-reversed channel response with the data sequence, which demands more computations than CPPUWB. Furthermore, prefiltering increases the dynamic range of the transmit signal, and TRP-UWB demands an more expensive linear amplifier to avoid signal saturation than CPPUWB. At the receiver end, despreading is needed in TRP-UWB for symbol decoding. In contrast, the peak received signal for each transmit symbol is sampled and then decoded in CPPUWB. It

is clear that CPPUWB is computationally more efficient than TRP-UWB.

- **High data transmission rate**

The proposed CPPUWB system encodes every transmit symbol with a specific channelized codeword  $\mathbf{c}$ . If we have a good estimate of the channel phase, a strong peak is expected due to the coherent combination of all multipath components. The power concentration of the received signal will mitigate the possible ISI from neighboring symbols, too. If ISI is sufficiently small, we can reduce the symbol interval to achieve a higher data transmission rate with respect to a fixed noise margin.

- **Secure data transmission**

It has been demonstrated in [9] that the spatial correlation between two UWB channels is less than 10% if they are separated by more than 10 inch. In other words, the transmit signal experiences independent channels at receivers in different locations. Since the codeword generated by the channel is random in nature, it makes eavesdropping more challenging. Under the same transceiver architecture, the eavesdropper will encounter serious ISI since the received signal is detected in a different location. Thus, the CPPUWB system can be used for secure data communication.

#### V. SIMULATION RESULTS

##### Example 1. Phase estimation

In this example, we evaluate the performance of the phase estimation scheme presented in Sec. II. The system parameters are  $L = 240$ ,  $\Delta = 0.5$  ns and  $\Gamma = 20.5$  ns (with the CM3 model) [7]. We evaluate the output SNR at  $r_{L-1}(i)$  as a function of input SNR parameterized by two different numbers of training symbols; namely,  $N = 100$  and 150. The results are shown in Fig. 2. We see that the output SNR performance improves as the number of training symbols or the input SNR increases. Also, the lower bound becomes tighter as SNR goes up. This is because the upper bound for  $Q(x)$  becomes tight as  $x$  increase. Also, Fig. 2 reveals the maximum number of training symbols required to achieve a certain performance level for different input SNR values. Therefore, the possibility of excess training is reduced, and a higher data rate can be achieved.

##### Example 2. BER Performance Evaluation

In this example, we compare the BER performance of the single-user, direct-sequence UWB (DSUWB) system [10] with the proposed CPPUWB scheme at two different data rates; namely, 25 Mbps and 50 Mbps. The system parameters are the same as those in Example 1. For the CPPUWB schemes, we consider two receivers: the receiver based on the sign of the estimated symbol and the MMSE receiver. The symbol intervals in our example are 80 and 40 chips for the data rate at 25Mbps and 50Mbps, respectively. The results shown in Fig. 3 are obtained by averaging over 1000

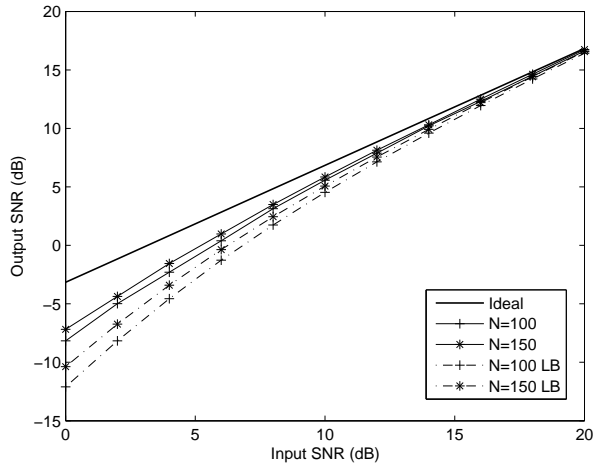


Fig. 2. The output SNR as a function of the input SNR parameterized by two different numbers of training pulses ( $N=100$  and  $150$ ), where LB denotes the lower bound of the output SNR performance.

channel realizations. When the data rate is higher, more chips belonging to different transmit symbols overlap with each other. Consequently, there is a more serious ISI effect that degrades the system performance.

For the DSUWB system, the length of the spreading code is limited by the symbol interval. Thus, the maximal-length ( $m$ -) sequences of 63- and 31-chip long are adopted for 25Mbps and 50Mbps, respectively. A selective RAKE (S-RAKE) [11] receiver that combines the strongest 15 taps is utilized to decode the transmit symbol. The channel estimation task is assumed to be perfect in DSUWB. For the proposed CPPUWB system, the fed back phase information is assumed to be perfect, too. It turns out that DSUWB and CPPUWB with the simple sign-based receiver render similar performances. Their curves overlap with each other and are difficult to differentiate in the figure. However, the system complexity for both schemes is quite different. To suppress the residual ISI, the MMSE receiver is applied to boost the system performance at the cost of higher receiver complexity. It gives the best performance. The curves are denoted by CPPUWB/MMSE.

## VI. CONCLUSION AND FUTURE WORK

The proposed CPPUWB system that utilizes the feedback channel phase information to encode the transmit data symbol was proposed in this work. It is more efficient than the conventional TRPUWB system in computation and power aspects. Since the phase estimation may not be perfect, we analyzed the system performance with contaminated phase information and derived a lower bound on the output SINR, which matched simulation results well when the input SNR is high. As shown in simulation results, the proposed CPPUWB system achieves a similar performance as DSUWB system with 15 RAKE fingers. However, the complexity is much reduced in the CPPUWB system. When the data rate is high, more serious ISI will occur. Our simulation results showed that the MMSE receiver can significantly improve the performance

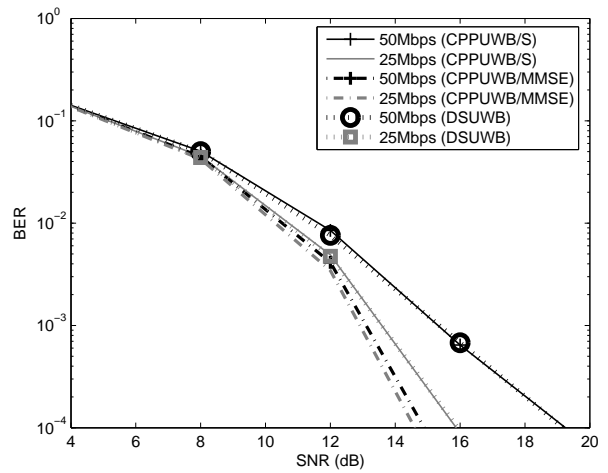


Fig. 3. The BER performance as a function of SNR for three systems with two different data rates: DSUWB, CPPUWB/S, CPPUWB/MMSE.

of CPPUWB at a higher computational cost at the receiver side.

An alternative for ISI suppression without demanding a high computational cost is to optimize the codeword length. Also, CPPUWB can potentially offer a flexible data rate and provide a secure data transmission. These will be our future research topics.

## REFERENCES

- [1] M. Z. Win and R. A. Scholtz, "On the energy capture of ultrawide bandwidth signals in dense multipath environments," *IEEE Communications Letters*, vol. 2, no. 9, pp. 245–247, Sept. 1998.
- [2] T. Strohmer, M. Emami, J. Hansen, G. Papanicolaous, and A. J. Paulraj, "Application of time-reversal with MMSE equalization to UWB communications," in *Proc. IEEE Globecom*, vol. 5, pp. 3123–3127, Nov. 2004.
- [3] V. Lottici, A. D'Andrea, and U. Mengali, "Channel estimation for ultra-wideband communications," *IEEE Journal on Selected Areas in Communications*, vol. 20, no. 9, pp. 1638–1645, Dec. 2002.
- [4] S. Niranjayan, A. Nallanathan, and B. Kannan, "Delay tuning based transmit diversity scheme for TH-PPM UWB: performance with RAKE reception and comparison with multi RX schemes," in *Proc. Joint UWBST & IWUWBS*, pp. 341–345, May 2004.
- [5] D. Cassioli, M. Z. Win, and A. F. Molisch, "The ultra-wide bandwidth indoor channel: from statistical model to simulations," *IEEE Journal on Selected Areas in Communications*, vol. 20, no. 6, pp. 1247–1257, Aug. 2002.
- [6] IEEE 802.15 high rate alternative PHY task group (TG3a) for wireless personal area networks (WPANs) <http://www.ieee802.org/15/pub/TG3a.html>.
- [7] Y.-L. Chao and R. A. Scholtz, "Weighted correlation receivers for ultra-wideband transmitted reference systems," in *Proc. IEEE Globecom*, vol. 1, pp. 66–70, Nov. 2004.
- [8] A. J. Viterbi, *CDMA: Principles of spread spectrum communication*. Reading, MA: Addison-Wesley, 1995.
- [9] C. Prettie, D. Cheung, L. Rusch, and M. Ho, "Spatial correlation of UWB signals in a home environment," in *Proc. IEEE UWBST*, pp. 65–69, May 2002.
- [10] J. R. Foerster, "The performance of a direct-sequence spread ultrawideband system in the presence of multipath, narrowband interference, and multiuser interference," in *Proc. IEEE UWBST*, pp. 87–91, May 2002.
- [11] M. Z. Win and R. A. Scholtz, "Characterization of ultra-wide bandwidth wireless indoor channels: a communication-theoretic view," *IEEE Journal on Selected Areas in Communications*, vol. 20, no. 9, pp. 1613–1627, Dec. 2002.